Atmospheric Environment Vol 15, No 6, pp 1035–1046, 1981
Printed in Great Britain

0004-6981/81/061035-12 $02.00/0
© 1981 Pergamon Press Ltd

OBJECTIVE ANALYSIS OF AIR POLLUTION MONITORING NETWORK DATA; SPATIAL INTERPOLATION AND NETWORK DENSITY

N. D. VAN EGMOND and D. ONDERDELINDEN
National Institute of Public Health, P.O. Box 1, Bilthoven, the Netherlands

(*First received* 5 *August* 1980 *and in final form* 7 *November* 1980)

Abstract—To obtain meaningful interpretations of the results of fixed air pollution monitoring stations, quantitative information on the spatial representativity of these results is of crucial importance. On the basis of data of the Dutch Air Pollution Monitoring Network a study was undertaken to estimate the absolute and relative errors which are involved in extrapolating the results beyond the actual spatial argument of measurement. In the first place, three interpolation techniques, optimum interpolation, eigenvector interpolation and so called distance-density interpolation, were compared for SO_2, NO, NO_2 and O_3. The differences between the results of these techniques proved to be small. It was further concluded that the interpolation errors and the associated persistence in space and time, as given by mutual correlations, should be specified with respect to pure space- or space-time variability. In the second place, the interpolation errors were generalized to other network densities on the basis of the optimum interpolation scheme and empirical observations. From the resulting relation between interpolation error and network density it was concluded that the SO_2-network of 108 stations over the measurement area of $150 \times 220\,km^2$ results in relative errors of 20%, small enough to detect mesoscale transports downwind of major source areas. The effect of sampling error, i.e., the small scale influences of local sources combined with the effect of measurement error, appeared to be of overriding importance in the efficiency of reconstruction of pollutant concentration fields at a given confidence level from monitoring network data.

1. INTRODUCTION

Among the objectives which are generally given for air pollution monitoring networks two main categories can be distinguished:

(a) the verification of physical and/or chemical models describing the transport and conversion of pollutants in the atmosphere and

(b) the description of the air pollutant concentrations in space and time, in the first place for control of levels with respect to public health standards.

In the first group of objectives additional information is introduced in the data-interpretation, e.g., in the form of a Gaussian plume model. For the second category in most cases the interpretation is based only on the measurement data obtained from a network. As pointed out very strongly by Goldstein and Landovitz (1977), this might be complicated by the failure of the fixed monitoring station to represent the pollution in a wider area. In that case no meaningful statements can be made about the pollutant concentration beyond the actually measured spatial arguments. For the evaluation of fixed monitoring network data in terms of space-time behaviour of the pollutant under study, two related questions thus have to be answered:

(a) Does the spatial representativity of the data permit a reconstruction of the underlying concentration field within given limits of error?

(b) If this is not the case, can statements be made about the dimensions of the area in which the measurement result of a single station may be considered as meaningful?

If the reconstruction of the field is found to be possible, the network might be considered as giving space-resolved information. If not, the network consists of a number of individual stations which have to be related separately to their respective small scale "areas of influence".

The objectives given above also apply to the National Air Pollution Monitoring System in the Netherlands; the spatial and temporal behaviour of SO_2, NO, NO_2 and O_3 should be given both on the mesoscale ($150 \times 220\,km$) by means of a 100 station baseline-grid (for SO_2), and on the small (urban) scale by additional 120 (SO_2-) stations. On both scales space-resolved interpretations are required for verification of models and testing public health criteria. Consequently, a study on interpolation techniques and representativity was undertaken resulting in an evaluation of the errors involved and in the choice of an interpolation procedure for (standardized) objective spatial analysis.

The investigations started from the Optimum Interpolation scheme which is widely applied in meteorology and is described by Gandin (1963), Alaka (1970) and Julian and Thiebaux (1975). In earlier work (Van Egmond and Tissing, 1977) eigenvector analysis was introduced in optimum interpolation to modify the covariance-structure which should be incorporated in the optimum interpolation scheme. With respect to empirical correlations fundamental problems were recognized in the application of optimum interpolation and consequently experiments were made with an interpolation procedure which was fully based on

eigenvector analysis of the empirical correlation (covariance) structure. For operational applications also a simple, pure analytical interpolation technique was developed. The empirical interpolation errors for these three interpolation schemes were evaluated and compared to "theoretical" ones, obtained from an assumed spatial correlation structure. Finally, the dependence of interpolation errors on network density is discussed.

2. INTERPOLATION SCHEMES

2.1. *Optimum interpolation (OI)*

For reconstruction of the two-dimensional concentration field at time t the pollutant concentrations C_{0t} at an array of non-station positions are estimated from linear combinations of the concentrations measured at surrounding monitoring stations. This procedure is called optimum interpolation if the weighting coefficients p_{i0} of the linear combinations are chosen in such a way that the discrepancy between estimated and true concentrations, the interpolation error E_{0t}, is minimal in the sense of least squares. However, the true concentrations have to be distinguished from measured values as the measurements are affected by errors. Further pollution concentrations might be influenced strongly by local sources resulting in substantial differences in measurement values for stations which are close together; in practice this small scale effect cannot be distinguished from measurement error. In order to account for these effects a sampling error h is introduced and for N surrounding stations the concentration C_{0t} then is written as

$$C_{0t} = \sum_{i=1}^{N} p_{i0}(C_{it} + h_{it}) + E_{0t} \tag{1}$$

where C_{it} is the true concentration at station i and time t, h_{it} the sampling error and $C_{it} + h_{it}$ the concentration measured at station i and time t. The coefficients p_{i0} are found from minimization of the squared interpolation error E_{0t} over a number of realisations, for example a sequence of T hourly concentrations.

Apart from the introduction of the constraint $\Sigma p_{i0} = 1$, as described in the Appendix, the coefficients finally are found from

$$\mathbf{p}_0 = (\mathbf{R} + \mathbf{I}\eta^2)^{-1}\mathbf{r}_0. \tag{2}$$

$\mathbf{R}$ is the $N \times N$ matrix of second moments ('correlations') between the N monitoring stations and $\mathbf{r}_0$ is the vector of expected correlations between the interpolation position and the N monitoring stations. To estimate these correlations homogeneity and, for convenience, isotropy will be assumed. Three types of correlations will be used to describe the field characteristics, i.e., $r_{i.}$, $r_{.t}$ and $r_{..}$ defined as the second moments about respectively the temporal (station) mean $M_{i.}$, the spatial mean (at time t) $M_{.t}$ and the space-time mean $M_{..}$. The sampling error h and interpolation error E will be normalized by division through the variances about these three first moments (mean-values) obtaining the normalized errors η and ε respectively.

In air pollution applications, high correlations can be expected for stations which are far apart, but sited in a comparable emission configuration, e.g., for two cities. In that case local emission characteristics might be the overriding influence of the concentration variability, resulting in extreme inhomogeneities; the high correlation cannot be generalized to other, particularly smaller distances, as they arise from two separate (time dependent) events instead of spatial field characteristics.

High mutual correlations lead to ill-conditioning of the empirical matrix $\mathbf{R}^m$. This results in computational instability when $\mathbf{p}_0$ is obtained from the empirical matrix $\mathbf{R}^m$. To overcome these difficulties the correlations might be described by an analytical model which is fitted to the empirical correlations given by $\mathbf{R}^m$; the modeled correlations then are inserted in the matrix $\mathbf{R}$ in Equation 2. However, as the required assumptions of homogeneity and isotropy in that case are rather stringent, an eigenvector interpolation scheme is introduced, which fundamentally accounts for high mutual correlations (ill-conditioning) without the stringent assumptions about homogeneity and isotropy.

2.2. *Eigenvector interpolation (EI)*

In eigenvector interpolation the correlations $\mathbf{r}_0$ are derived from the local statistical characteristics of the field, avoiding unjustified assumptions about homogeneity and isotropy. As described in the Appendix, the coefficients p_{0i} are found as a linear combination of the eigenvectors $\mathbf{e}_k$ of the matrix of empirical covariances, only taking into account the L vectors with eigenvalues larger than the squared sampling error ($\lambda \gg h^2$):

$$\mathbf{p}_0 = \sum_{k=1}^{L} \frac{\lambda_k}{(\lambda_k + h^2)} e_{k0}\mathbf{e}_k \tag{3}$$

where the coefficients e_{k0} are the local values of the spatial eigenvector patterns, obtained by some arbitrary (analytical) interpolation. As vectors with smaller eigenvalues are not taken into account, computational instability due to high mutual (empirical) covariances (correlations) is essentially avoided in this scheme.

2.3. *Distance and density weighting function interpolation (DDI)*

The introduction of modelled spatial correlations results in the optimum interpolation scheme in coefficients p which only are dependent on the distance between gridpoint and observation positions (as given by $\mathbf{r}_{i0}$ in Equation (2)) and the mutual distances between the monitoring stations (as given by the correlations $\mathbf{R}$ in Equation (2)).

Considering the computational efforts which are involved with optimum interpolation, a third scheme was introduced. Herein the coefficients p_{i0} are simply

determined by both distance and local network density, according to analytical weighting functions. The scheme can be applied to a single realisation of the concentration field and is arbitrary in character:

$$p_{i0} = \frac{\exp(-x_{i0}/A)/D_i}{\sum_{j=1}^{N} \exp(-x_{j0}/A)/D_j} \quad (4)$$

where A is a specific distance which is chosen in dependence of the statistical structure of the field, x_{i0} is the distance between grid- and observation position and D_i is the network density at station i, defined by

$$D_i = \sum_{j=1}^{N} \exp(-x_{ij}/A_d)$$

where x_{ij} is the distance between station i and surrounding stations j and A_d a specific distance which defines the area in which the monitoring stations have density weights which sum up to '1' and thus are weighted as a single observation. The station itself is included in the summation ($j = i$) and a single station i in an area with radius $\gg A_d$ will thus have $D_i = 1$.

3. EXPERIMENTS

3.1. *Data*

The computational experiments were based on the measurement results of the baseline-grid (background) stations of the Dutch Air Pollution Monitoring Network, which comprises 108 stations for SO_2, a subset of 44 stations for NO and NO_2 measurement, and a subset of 28 stations for the measurement of the O_3-concentrations. The measurement area ($\pm$ 33.000 km^2) covers the total area of the Netherlands (150 x 220 km). The concentrations are measured continuously and after data-validation hourly average values are formed. The following instruments are used:

SO_2	Philips PW 9700 (upgraded)	coulometry
NO, NO_2	Philips PW 9762/00	chemiluminescence
O_3	Philips PW 9771/00	chemiluminescence

The instruments for SO_2 and NO, NO_2 are calibrated every 24 h and the O_3-monitor every measuring cycle of 80 s.

The performance of the three interpolation techniques was evaluated on the basis of hourly values of SO_2, NO and NO_2 over the January and February 1979 period, which was characterized by high pollutant concentrations due to frosty weather conditions resulting in an increase of emissions (lower ambient temperatures) and a deterioration of atmospheric dispersion conditions. For computations on O_3 the results of June 1979 were used, ensuring sufficient spatial and temporal variability. For practical reasons some computations with respect to SO_2 had to be limited to the number of 44 (NO_x-subset) stations.

3.2. *Correlation structure*

The 'correlations' r_{ij} which were introduced above, should be derived from the records of observations of monitoring stations. From the SO_2 hourly concentration records of 44 stations over a two-month period empirical correlation functions r^m, r_t^m and r_i^m with respect to the overall constant mean M, the hourly mean field M_t and the station means M_i were computed; the functions are presented in Fig. 1. As a consequence of sampling error in the measured concentrations, all correlation functions exhibit correlations $r_0^m < 1$ at extrapolation to zero (interstation) distance. The empirical correlations are related to the true concentrations; for example

$$r_{ij}^m = \frac{\overline{C_{it}C_{jt}} + \overline{h_i^2}\,\delta_{ij} - M^2}{\overline{C_{0t}^2} + \overline{h_t^2} - M^2}$$

with $\delta_{ij} = 1$ for $i = j$ (zero interstation distance) and $\delta_{ij} = 0$ otherwise, from which η^2 is obtained as

$$\eta^2 = \frac{(1 - r_0^m)}{r_0^m} \quad (5)$$

From Fig. 1 η^2 and η_t^2 are estimated within the range of 0.05–0.10 and η_t^2 is estimated between 0.10 and 0.15.

The function r_t^m indeed can be derived from the functions r^m and r_i^m by application of Equation (A6) (and accounting for sampling error); as the variances are related by $\overline{(C_t - M)^2} \simeq 2\overline{(M_t - M)^2}$ a value of for example $r^m = 0.70$ (at $\pm$ 50 km) results in $r_t^m = 0.37$, in agreement with Fig. 1.

The function r_i^m shows negative values for larger distances, indicating that spatial trends affect the correlation structure; alternatively the correlations r_{xt} with respect to the trend surface M_{xt} could have been used. As primarily the correlation behaviour near the origin is relevant in the computations, a simple positive

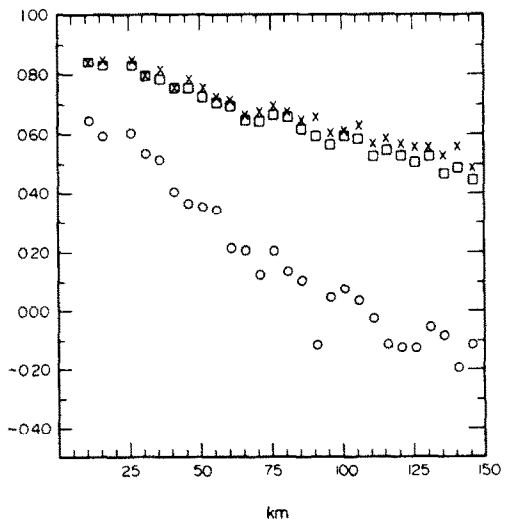

Fig. 1. Spatial correlation functions r_t^m(×), r^m(□) and r_i^m(○) for hourly SO_2-concentrations (Jan.–Feb., 1979).

definite analytical function was used to describe the (true) spatial correlation structures:

$$r(x) = \exp\left(-\frac{x}{A_0}\right) \tag{6}$$

where A_0 is the correlation distance and x the (non-directional) spatial argument.

The correlation functions for SO_2, NO_2 and O_3 show high spatial persistence (positive correlations over larger distance), which is explained from the fact that for these components, and during the winter months, even for NO, large scale fluctuations are generated by mesoscale transport.

3.3. *Eigenvector analysis*

In the EI-scheme the correlation (covariance) structure is given by the eigenvectors of the empirical (covariance) matrix S^m. Inspection of the vectors and the corresponding eigenvalues gives insight in the spatial scale of the (temporal) fluctuations over the field. Small scale variability is characterized by sign reversals on the eigenvector elements of nearby stations and should be excluded from the linear combinations 3. As a measure for this, the quantity

$$q_k = \frac{(e_{k0} - \hat{e}_{k0})^2}{e_{k0}^2}$$

is taken from Equation (A9) and computed for all 44 stations for which eigenvector analysis was made, on the basis of the variances $\overline{(C_t - M_{..})^2}$ and $\overline{(C_t - M_{.t})^2}$; the variances with respect to $M_{t.}$ are about equal to those with respect to $M_{..}$, having about the same correlation structure (Fig. 1), and were not taken into account. The local interpolations were made by application of the DDI-scheme (Equation 4).

Analysis for $M_{..}$ resulted in a first vector explaining 60% of the total variance (relative to $M_{..}$) showing a large scale south–north trend, in agreement with the variance of the time variability of the spatial mean $\overline{(M_{.t} - M_{..})^2}$ which explains about 50% of the variance $\overline{(C_t - M_{..})^2}$. Thirteen vectors explain 95% of the total variance, the latter vectors having $q_k > 1$, indicating small scale variability. The sampling error fraction $\eta_{..}^2$ is thus estimated in the order of 0.05–0.10 in agreement with the estimate from the correlation functions. An example of a vector with $q_k > 1$ is given by vector 7 in Fig. 2, explaining only 1% of the total variance. In several parts of the field strong gradients occur on sub-network scale but in large areas vast zones of positive or negative values are observed, illustrating that the eigenvector analysis does not necessarily give an efficient separation in small scale and large scale effects.

The analysis of the variance–covariance pattern $\overline{(C_t - M_{.t})^2}$ results in an explained variance of 87% for 13 vectors and thus in an indication of $\eta_{t.}^2 = 0.10$–0.15.

3.4. *Sampling error*

From both the correlation structure and the eigenvector-analysis estimations of $\eta^2 = 0.05$–0.10 and

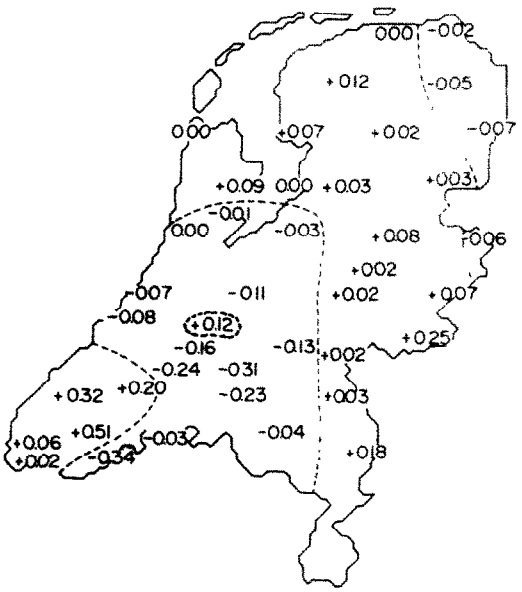

Fig. 2. 7th eigenvector pattern for SO_2 (Jan.–Feb., 1979); $\langle q_7 \rangle = 110\%$, explained relative variance 2%.

$\eta_{t.}^2 = 0.10$–0.15 were obtained. A third possibility of estimating η^2 is given by the direct intercomparison of observation records of stations which are sited close together. Assuming again that the sampling errors are uncorrelated and equal in magnitude, $\overline{h_t^2}$ can be estimated from the squared differences of the measured concentrations $C_{it} + h_{it}$ and $C_{jt} + h_{jt}$ at small interstation distances x_{ij}. Dividing by the (true) variances, η^2 are obtained. For two SO_2-stations with $x_{ij} = 0.3$ km $\eta_{..} \simeq \eta_{i.} = 0.34$. In the same area a value $\eta_{i.} = 0.29$ was found for $x_{ij} = 3$ km. As herein also a pure interpolation error must be present, a value of $\eta_{..} = \eta_{i.} = 0.25$ finally was assumed in the interpolation computations. In the same way the sampling error with respect to the variance $\overline{(C_t - M_{.t})^2}$ was estimated; $\eta_{.t} = 0.34$.

3.5. *Intercomparison of interpolation schemes*

For intercomparison of the three interpolation schemes the hourly average concentrations at a set of test-stations were computed from several configurations of network stations over 1416 h of January and February 1979 for SO_2, NO_2 and NO, and 720 h of June 1979 for O_3; measurement set (44 stations) and test set (15 stations) for SO_2 are given in Fig. 3. To allow further comparisons these configurations were chosen to correspond as closely as possible to the rectangular measurement-teststation configuration with grid-length x_0 given in Fig. 7; the 44 station-network has a gridlength $x_0 = 40$ km. The results are presented as absolute ($\sqrt{\langle E_k^2 \rangle}$) and normalized ($\sqrt{\langle \varepsilon_k^2 \rangle}$) interpolation errors, uncorrected for the sampling errors h at the test-stations. To obtain the

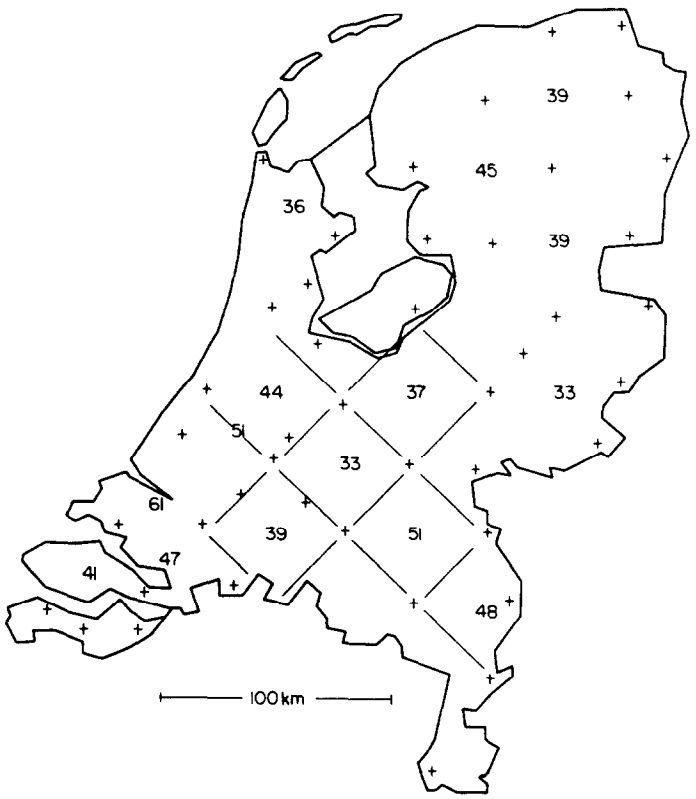

Fig. 3. Measurement set with $x_0 = 40$ km (44 stations) and uncorrected errors $\varepsilon_{hi.}$ at test-positions for SO_2 (Jan.–Feb., 1979).

pure (empirical) normalized interpolation errors, ε_h^2 should be reduced by η^2 according to

$$\varepsilon^2 = (1+\eta^2)\,\varepsilon_h^2 - \eta^2 \qquad (7)$$

The interpolation errors $\varepsilon_{hi.}$ were computed for a wide range of specific distances A (EI-and DDI-schemes) and correlation distances A_0 (OI-scheme). The results for SO_2 are given in Fig. 4. The profile for optimum interpolation ($\varepsilon_h = \varepsilon_{hi.}$) is rather flat over the range $A_0 = 40$–600 km. This is explained from the nature of optimum interpolation where a higher (assumed) correlation distance (A_0) in the **R** matrix is compensated by the $\mathbf{r}_0$ vector (Equation 2) and consequently the coefficients $\mathbf{p}_0$ vary only slowly over this wide range. In the EI- and DDI-schemes this compensation is not provided and a more pronounced optimum is found at $A = 13$ km. It further should be noted that the covariance structure (persistence) in the EI is not really changed by varying A; only the DDI-interpolation, which is used in the EI-application to derive s_0, is smoother at larger A. EI strongly approximates DDI which indicates that the effect of filtering (smoothing) the empirical data by deleting several (small scale) vectors is small. To facilitate the interpretation of Fig. 4 the error E_h', obtained by multiplying $\sqrt{\langle \varepsilon_h^2 \rangle}$ by the square root of the uncorrected variance $\overline{(C_{ii} + h_{ii} - M_i.)^2}$, is given on the right ordinate. The

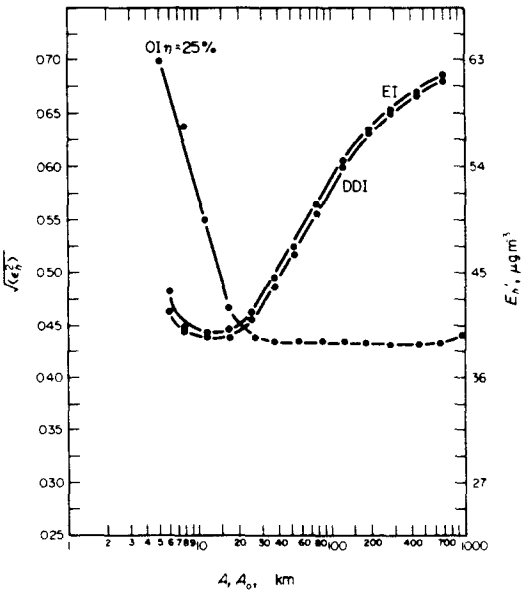

Fig. 4. Interpolation errors $\sqrt{\langle \varepsilon_h^2 \rangle}$ and E_h' as functions of correlation distance A_0 for optimum interpolation (OI–25%) with $\eta = 0.25$, as function of A for both distance-density interpolation (DDI) and eigenvector interpolation (EI); SO_2, Jan.–Feb., 1979.

Table 1 Absolute and relative errors for optimum interpolation (OI), eigenvector interpolation (EI) and distance density interpolation (DDI), for the components SO_2, NO_2, NO and O_3.

					Absolute and normalized errors						Relative errors	
	N_{meas}	N_{test}	x_0, km		$\sqrt{\langle E_k^2 \rangle}$, $\mu g/m^3$	$\sqrt{\langle \varepsilon_k^2 \rangle}$	$\sqrt{\langle \varepsilon^2 \rangle}$	η_t.	A_0, km	M_t. $\mu g/m^3$	$\sqrt{\langle F_k^2 \rangle}$	$\sqrt{\langle F^2 \rangle}$
SO_2	44	15	40	OI	38.8	0.43	0.37	0.25	170	92	0.33	0.28
				EI	40.0	0.44	0.38	0.25	13	92		
				DDI	38.7	0.43	0.37	0.25	13	92	0.33	0.28
	93	15	28	DDI	36.9	0.41	0.34	0.25	13	97	0.30	0.25 ($h_f = 0.17$)
NO_2	30	13		OI	12.5	0.50			200	47	0.31	0.28
				EI	12.4	0.48			17	47		
				DDI	12.8	0.53			25	47	0.30	0.27
	45		40	theor.								0.22
NO	30	13		OI	17.9	0.59			120	30	0.49	0.41
				EI	19.3	0.65			10	30		
				DDI	18.2	0.64			15	30	0.44	0.35
	45		40	theor.								0.45
O_3	18	7		OI	18.0	0.20			280	78	0.28	0.27
				EI	18.2	0.20			28	78		
				DDI	18.3	0.22			32	78	0.28	0.27

interpolation errors at the optimum value of A_0 and A for the three techniques and the four components are given in Table 1. The differences between the techniques are extremely small. The errors ε_{hi}. for SO_2 are given at the test-station positions in Fig. 3. It is concluded that for practical applications the relatively simple DDI-scheme gives satisfactory results. However, for generalizations of interpolation errors the OI-scheme should be used because of its ability to give a direct relation both between spatial persistence (A_0) and interpolation error ε, and between network density and interpolation error, as will be shown later.

To estimate the effective correlation distances of the structures ($r..$, $r_{i.}$ and $r_{.t}$) the 'theoretical' errors $\varepsilon_{i.}$ and $\varepsilon_{.t}$ are computed directly from Equation (A4) after substitution of the 'true' correlations, described by Equation (6) for a range of A_0 values in Equation (A3). Then the values of A_0 can be determined for which these theoretical errors equal the empirical errors. In this way correlation distances A_0 for $r_{i.}$ and $r_{.t}$ were found to be respectively 170 km and 50 km for SO_2 which is in agreement with the empirical correlation functions presented in Fig. 1. The value for $r_{i.}$ approximately equals that of $r_{..}$. It is concluded that the empirical correlation functions can be directly related to interpolation errors. As the variances about $M_{i.}$ at the testset stations amounts more than two times the variance about $M_{.t}$, the reduced error $\varepsilon_{.t} = 0.66$ is substantially larger than $\varepsilon_{i.}$, and this illustrates the importance of specifying correlation distance (persistence) in terms of the variance considered; when time variance is included a much larger "spatial" persistence r and r_t is observed than in the case of restricting the analysis to pure spatial variability ($r_{.t}$).

The errors for NO_2, NO and O_3 are given in Table 1. Estimation of sampling errors from the less dense networks is hardly possible and, consequently, only uncorrected interpolation errors are presented. The errors for NO are large ($\varepsilon = 0.59$) and the correlation distance is relatively short. For comparison of theoretical and empirical errors a value of $A_0 = 120$ km was found, in agreement with the NO correlation function r_t from which a least squares fit of the analytical function in Equation (6) resulted in $A_0 = 136$ km. The A_0-values for all components, assuming $\eta_{i.} = 0.25$ are given in Table 1.

Finally, in Fig. 5 an example is given of SO_2-concentration fields as reconstructed by the three interpolation techniques. The DDI-scheme is applied to sets of both 44 and 108 stations. The EI- and OI-fields both are based on the measurement set of 44 stations, which has been depicted in Fig. 3. The EI-scheme does not fully reconstruct the mesoscale SO_2-plume, which is explained by the fact that the variance of these type of pronounced patterns is relatively small in comparison to the variance averaged over the two months period. Alternatively, eigenvectors over a shorter period of several days might have been used. The gradients in the OI-field are larger than in the DDI-field, inherent to OI in which negative coefficients for p_{0i} are allowed in contrast to DDI. The differences between the 108 and 44 stations network (DDI) are rather small.

3.7. *Relative errors*

The absolute errors E_h (Table 1) and the normalized errors ε_h cannot be easily interpreted. The distribution of individual errors, i.e, the discrepancies between interpolated and measured concentrations at test-stations, cannot be considered as obtained from a normal distribution; too many relatively small errors were found. Due to the lognormal nature of the underlying measurement results, the distribution of errors appears as the sum of a number of normal distributions with different variances. Furthermore a pronounced linear relationship was found between the station variances $\overline{(C_{it} - M_{i.})^2}$ and the station averages $M_{i.}$, also interpolation errors seem to be dependent on the measured concentration level and as a consequence the relative variance

$$\overline{\left(\frac{E_{0t}}{C_{0t}}\right)^2} = \overline{\left(\frac{\hat{C}_{0t} - C_{0t}}{C_{0t}}\right)^2}$$

is in principle statistically a more meaningful quantity to minimize. Herein $\hat{C}_{0t}$ is the value obtained by interpolation and again C_{0t} the true concentration. In order to evaluate the magnitude of this relative error and its dependence on spatial persistence, the same procedure as for the minimization of the absolute interpolation variance was applied to the logarithm of the measured concentrations. This is based on the approximation:

$$F_{0t} = \ln\hat{C}_{0t} - \ln C_{0t} \simeq \frac{\hat{C}_{0t} - C_{0t}}{C_{0t}}$$

A comparison of the empirical errors $\overline{F_h^2}$ and $\overline{(\hat{C}_{0t} - C_{0t}/C_{0t})^2}$ for SO_2-concentrations $C_{0t} > 30\,\mu g\,m^{-3}$ showed an excellent correspondence between the relative error and its approximation $\overline{F_h^2}$. Further, the differences between the values of $\overline{F_h^2}$ computed by the three techniques were small. The resulting relative errors are given in Table 1. The correlation structure of the logarithmic SO_2-levels, which is involved in the OI-scheme, gives a shorter correlation distance ($A_0 = 100$ km) than the linear correlation structure r_t^m, which has been given in Fig. 1. From this correlation function and from analysis of discrepancies between stations which are sited close together, the relative sampling error was estimated as $h_f = 0.17$. For monitoring stations in the vicinity of industrial sources higher values up to $h_f = 0.25$ were found.

For two network densities empirical relative errors were calculated, $F_h = 0.30$ at $x_0 = 28$ km and $F_h = 0.33$ at $x_0 = 40$ km. Correction for the sampling error $h_f = 0.17$ at the testset stations according to $F^2 = F_h^2 - h_f^2$ resulted in relative errors $F = 0.25$ at $x_0 = 28$ km and $F = 0.28$ at $x_0 = 40$ km. For $h_f = 0.25$

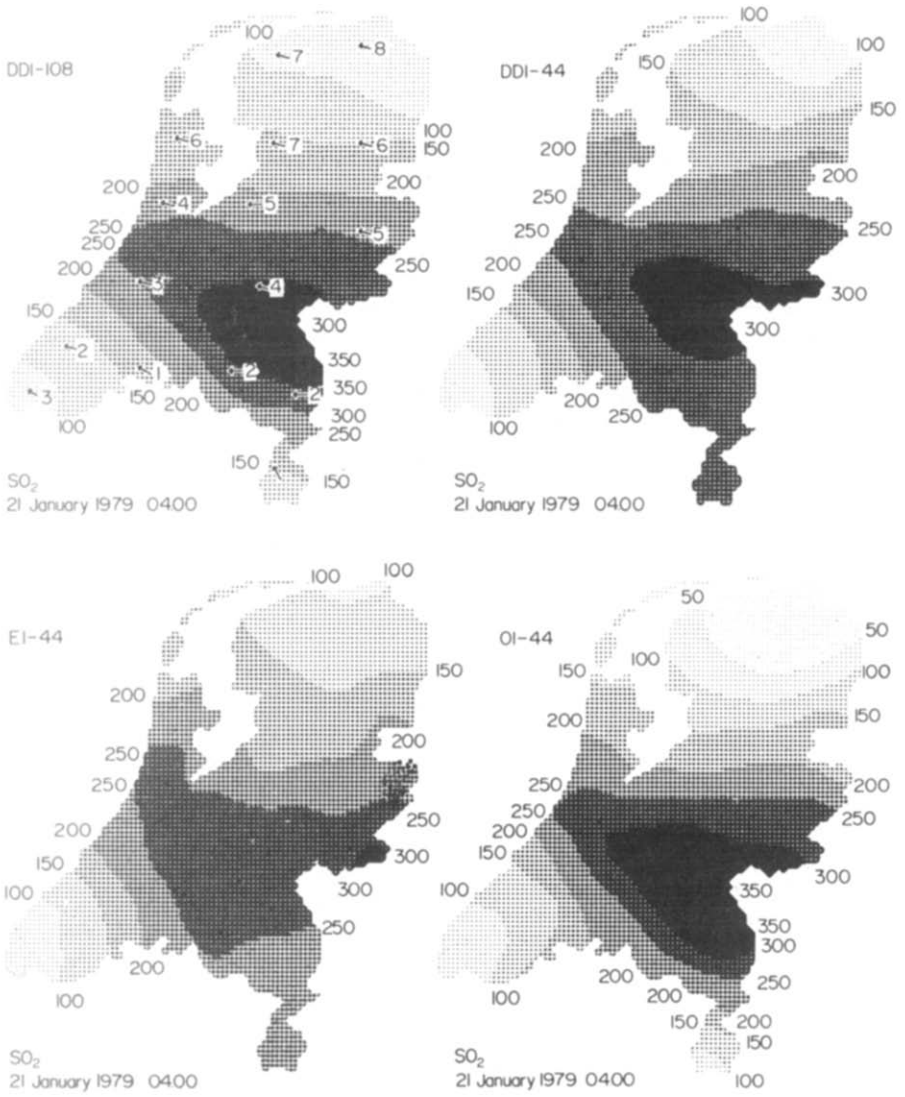

Fig. 5. Concentration fields in $\mu g\,m^{-3}$ for SO_2 on 21 January 1979, 04.00 for distance-density interpolation with 108 stations (DDI-108) and 44 stations (DDI-44), eigenvector interpolation (EI-44) and optimum interpolation (OI-44) both also with 44 stations.

values of respectively $F = 0.17$ and $F = 0.21$ were found. The distribution of uncorrected errors F_k for the network of 44 stations at 15 test stations is given in Fig. 6 and can be considered as a normal distribution.

The relative uncorrected errors F_k for the other pollutants are given in Table 1. Due to the larger uncertainty in the estimate of sampling error, the corrected values F have to be considered as first estimates. For NO_2 and NO the relative theoretical errors, computed in the same way as for SO_2, are $F = 0.22$ and $F = 0.45$ respectively ($x_0 = 40$ km, 45 stations).

4. NETWORK CONSIDERATIONS

From comparison of the 'theoretical' errors with empirical errors, corrected for the sampling errors at test-stations, correlation distances A_0 were found which correspond to the empirical SO_2-correlation functions. Applying the theoretical optimum interpolation scheme, given by the Equations (A3) and (A4) for these correlation distances in the network configuration given by Fig. 7, the empirical corrected interpolation errors $\varepsilon_{i.}$, $\varepsilon_{.t}$ and E can be generalized to other network densities (interstation distances) than that of the experimental configuration with $x_0 = 40$ km (Fig. 3) from which the empirical errors were obtained. For SO_2 the theoretical error E, which equivalently can be obtained from $\varepsilon_{i.}$ with $A_0 = 170$ km, $\eta = 0.25$ or $\varepsilon_{.t}$ with $A_0 = 50$ km, $\eta = 0.34$ is given as a function of grid-length x_0 in Fig. 8. On the abcissa the numbers of grid-cells and the approximate numbers of stations N (including extra stations at the boundary) of the rectangular network are given. The dense SO_2-network permits a verification of these curves by

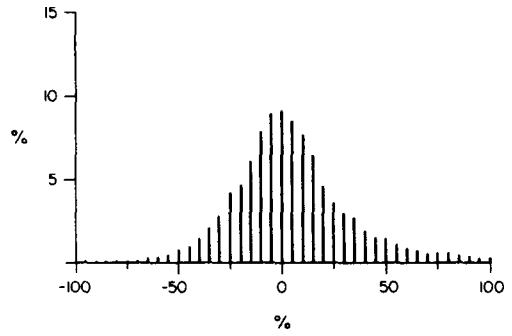

Fig. 6. Distribution of relative errors F_h for the SO_2-network with $x_0 = 40$ km (44 stations).

computation of the interpolation errors at the same 15 testset stations in a more dense configuration with $x_0 = 28$ km. These errors, again corrected for sampling error, are plotted in the same figure, together with the empirical errors at $x_0 = 40$ km. The empirical errors at $x_0 = 28$ km fit reasonably to the theoretical curves.

Application of the same procedure to the relative error F results in the relationships given in Fig. 9. Again the empirical errors at $x_0 = 28$ km (with $h_f = 0.25$ and $h_f = 0.17$) fit in the theoretical relation between relative error and network grid-length (network density). Extrapolation to $x_0 = 19$ km (108 stations) with $h_f = 0.25$ results in a relative interpolation error of about 0.15. This is smaller than the individual relative sampling error $h_f = 0.25$, as the interpolated value is found as a "weighted mean" from several surrounding stations. The sampling error $h_f = 0.17$ results in an extrapolated relative error $F = 0.20$ at $x_0 = 19$ km. The error of 15–20% allows significant detection of mesoscale plumes which affect the SO_2 concentration levels in the Netherlands and which show "plume"-axis concentrations of at least 40% higher than the background concentration, an example of which has been given in Fig. 5.

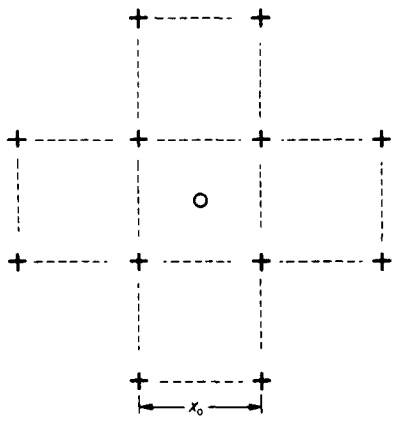

Fig. 7. Network configuration for theoretical computation of ε as a function of grid-length x_0, corresponding to the Dutch network in SE–NW orientation.

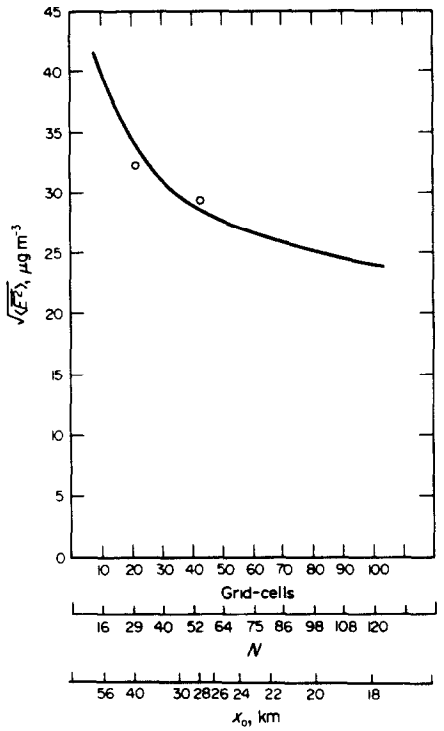

Fig. 8. Relation between absolute interpolation error E and grid-length x_0 with approximate number of network stations N. Empirical observations are given as dots.

5. CONCLUSIONS

(1) The differences between optimum-, eigenvector- and distance-density interpolation for reconstructing air pollution (mesoscale) concentration fields are small. For practical applications the more simple and efficient distance-density scheme can be used. For network considerations this scheme can be combined with the optimum scheme for describing the relationship between network density and spatial interpolation error, and for assessing the spatial meaning of fixed monitoring station data.

(2) As the use of different types of 'correlations' leads to large differences in normalized interpolation errors, these types of correlations should be specified in air pollution studies. Pure spatial persistence (correlation distance) appears to be much smaller than suggested by the conventional 'time-space' correlations. Consequently, interpolation errors expressed in terms of the pure spatial variability are much larger than the errors with respect to the variability of individual stations in time.

(3) The absolute interpolation error for SO_2 at the present network density with interstation distances of 19 km is estimated as $24\,\mu g\,m^{-3}$. At interstation distances of 40 km, this error amounts about $33\,\mu g\,m^{-3}$. The relative errors of the 108 stations SO_2-network are estimated to be 20%; the errors can be considered as

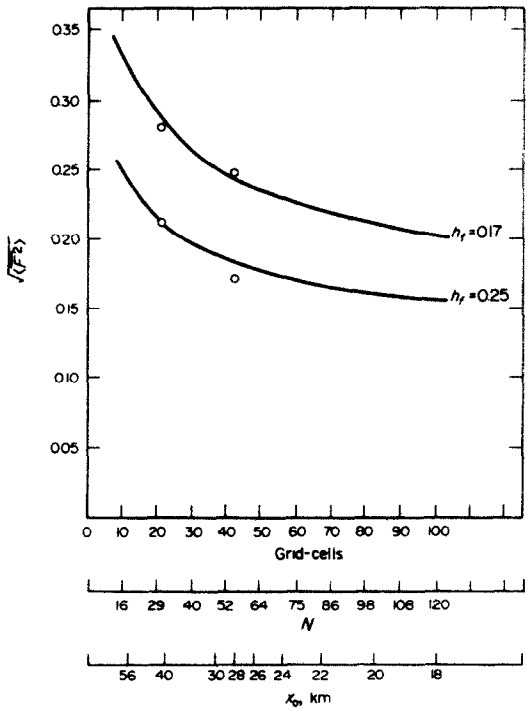

Fig. 9. Relations between relative interpolation error F and grid-length x_0 with approximate number of network stations N for $h_f = 0.25$ and $h_f = 0.17$. Empirical observations are given as dots.

being obtained from a normal distribution. The estimate is affected strongly by the value of sampling error, which only can be determined with low accuracy. The precise determination of sampling error needs further attention. The errors computed for NO are large and for the time being it is concluded that interpolation of the NO-concentrations only makes sense in exceptional cases. Precise estimation of NO-errors only can be made when better estimations of sampling error are available.

(4) The relative interpolation error for SO_2 at the network density $x_0 = 19$ km ($F = 20\%$) allows meaningful reconstruction of mesoscale plumes affecting the SO_2-concentration in the Netherlands, where inland and foreign source configurations are such that mesoscale plume-axis concentrations are more than 40% higher than 'background' concentrations. Spatial interpolations for NO_2 and O_3 can be made with small relative errors ($\pm 20\%$ at $x_0 = 40$ km) as the spatial variability of these components for an important part are generated by large scale transport.

Acknowledgement—The authors are grateful to O. Tissing and H. Kesseboom for the development of some of the computer programmes for this study and for their contributions to the development of operational interpolation and mapping techniques.

REFERENCES

Alaka M. A. (1970) Theoretical and practical considerations for network design. *Met. Monogr.* **11** (33), 20–27

Egmond N. D. van and Tissing O. (1977). Optimum interpolation of spatial air pollution data. *Proceedings IV Int. Clean Air Congres*, Tokyo, Japan pp. 658–662

Gandin L. S. (1965) Objective analysis of meteorological fields (translated from Russian) *Israel Progr. for Scient. Transl., Jerusalem*, No. 242.

Goldstein I. F. and Landovitz L. (1977) Analysis of air pollution patterns in New York City. I. Can one station represent the large metropolitan area? *Atmospheric Environment* **11**, 47–52.

Marquardt D. W. (1970) Generalized inverses, ridge regression, biased linear estimation and non linear estimation *Technometrics* **12**, 591–612.

Thiebaux H. J. (1974) Estimation of covariances of meteorological parameters using local time averages. *J. appl. Met.* **16**, 592–599

APPENDIX

Optimum interpolation

The concentration C_{0t} is obtained from the measured concentrations $C_{it} + h_{it}$ (true concentration and sampling error) at N surrounding monitoring stations according to

$$C_{ot} = \sum_{i=1}^{N} p_{i0} (C_{it} + h_{it}) + E_{ot} \qquad \text{(A1)}$$

The coefficients p_{i0} are found from minimization of the squared interpolation error E_{0t} over a number of realisations for example a sequence of T hourly concentrations:

$$\frac{1}{T} \sum_{t=1}^{T} E_{ot}^2 = \overline{E_{ot}^2} = \overline{\left[C_{0t} - \sum_{i=1}^{N} p_{i0} (C_{it} + h_{it}) \right]^2} \qquad \text{(A2)}$$

Although the contributions of local sources will always result in a positive effect, i.e., $\overline{h_i} > 0$, they will affect the monitoring stations at directions and conditions which vary strongly from station to station and time to time. It therefore is assumed that the sampling errors h are not correlated with each other and with the true concentrations. Lacking any information on the magnitude of sampling error at individual stations, it further is assumed that the mean squares of the errors are equal at all stations. $\overline{h_i^2} = \overline{h_{it}^2}$.

Introducing the normalized (squared) interpolation error ε and the normalized (squared) sampling error η.

$$\varepsilon^2 = \frac{\overline{E_{0t}^2}}{\overline{C_{0t}^2}} \qquad \eta^2 = \frac{\overline{h_i^2}}{\overline{C_{0t}^2}}$$

and writing

$$\frac{\overline{C_{it} C_{jt}}}{\overline{C_{0t}^2}} \text{ and } \frac{\overline{C_{it} C_{0t}}}{\overline{C_{0t}^2}} \text{ as } r_{ij} \text{ and } r_{i0} \text{ respectively,}$$

the coefficients p_{i0} are found by taking the N derivatives with respect to p_{i0} and equating the results to zero. Then the coefficients p_{i0} are found from the set of equations

$$\mathbf{p}_0 = (\mathbf{R} + \mathbf{I}\eta^2)^{-1} \mathbf{r}_0 \qquad \text{(A3)}$$

where $\mathbf{R}$ is the $N \times N$ matrix of (true) cross-products r_{ij}, $\mathbf{r}_0$ the vector of elements r_{i0} and $\mathbf{I}$ the unit matrix. The normalized error ε then is given by

$$\varepsilon^2 = 1 - \mathbf{r}_0 \mathbf{p}_0 \qquad \text{(A4)}$$

The coefficients p_{i0} thus are obtained from the quantities r_{ij} and r_{i0} which can be considered as the true "correlations" with respect to the zero-level. r_{ij} can be derived from the measured

"correlations" r^m_{ij} between stations i and j. For r_{i0} this is not possible as the values r^m_{i0} are not available, and r_{i0} consequently has to be deduced from the general behaviour of r_{ij} over the field. This requires the assumption of homogeneity, implying invariance of r_{ij} under translations. As for practical reasons also isotropy will be assumed, the values r_{ij} are taken to be only dependent on the distances between (station) positions i and j. Several possible first-moment fields or 'averages' M are examined, considering in particular the meaning of "spatial correlations" r_{ij} and the normalized errors ε.

The true concentration C_{it} is written as the sum of an average level M and a deviation of this level C'_{it}. Rewriting Equation (A1)

$$C'_{0t} + M = \sum_{i=1}^{N} p_{i0}(C'_{it} + M + h_{it}) + E_{0t} \qquad \text{(A5)}$$

and assuming, as motivated before, that the sampling errors h_{it} average out for the possible levels M, three mean levels M are considered:

(1) $M = \overline{\langle C_{it} \rangle}$; the overall space-time average concentration. In the special case that $\Sigma p_{i0} = 1$, M substituted in Equation (A5) cancels out and the coefficients p_0 are found from Equation (A3) with 'correlations' defined for the relative levels C'_{it} and C'_{0t}. The 'variance' $\overline{C'^2_{0t}}$ is unknown and should be approximated in practical applications by $\langle \overline{C'^2_{it}} \rangle$, i.e., the spatial mean of the variances at individual stations. This implies the assumption that the variances are constant over the field. The normalized interpolation error ε in this case applies to this variance, i.e., the second moment relative to the overall mean M.

(2) $M_t = \langle C_{it} \rangle$; the spatial mean field for hour t. Also in this case the coefficients are simply obtained from Equation (A3) under the constraint $\Sigma p_{i0} = 1$. The correlations r_{ij} thus are defined with respect to the hourly average field M_t. In case of a trend component the spatially constant level M_t might be replaced by a slowly varying trend surface M_{xt}, which changes r_{ij} only over larger distances and which can be considered as a combination of 'local'-average fields. The error ε_t gives the error with respect to the second moment relative to M_t, i.e., $\langle \overline{(C_{it} - M_t)^2} \rangle$.

(3) $M_i = \overline{C_{it}}$; the (time) average concentration at station i. The deviations $C_{it} - M_i$ are thus the normal deviations from the station mean concentrations. It can be shown that the coefficients p_{i0} can be obtained from the general solution Equation (A3) if $\Sigma p_i M_i = M_0$, which essentially assumes, as could be expected, that the interpolation of the deviations C'_{it} also holds for the mean (first-moment) values. This seems to be justified only for fields with weak gradients in the average values. The corresponding normalized error will be denoted by ε_i. The correlations r, r_t and r_i thus, defined as the normalized cross-products of deviations from respectively M, M_t and M_i, are related representations of the given statistical structure of the pollutant under study over the field. When for example the correlation r is given, the correlation r_t can be computed from

$$r_t = \frac{r\,\overline{(C_{0t} - M)^2} - \overline{(M_t - M)^2}}{\overline{(C_{0t} - M)^2} - \overline{(M_t - M)^2}} \qquad \text{(A6)}$$

The variance $\overline{(C_{0t} - M)^2}$ can be approximated by the spatial mean $\langle \overline{(C_{it} - M)^2} \rangle$ of the variances of individual stations with respect to M; the quantity $\overline{(M_t - M)^2}$ is the second moment (variance) of the hourly (spatial) mean level M_t relative to the overall space-time mean M. In comparing measured correlations r^m_t and r^m the true variance $\overline{(C_{0t} - M)^2}$ should be replaced by the measured variance $\overline{(C_{0t} + h_{0t} - M)^2}$. More general the correlation function r can be considered as the sum of several correlation functions with different correlation distances, resulting from independent sources of variability with different spatial scales. The level M_t is a particular representation of the variability resulting from large scale time fluctuations, with correlation functions $r(x) = 1$ for all x. According to Equation (A6) r is a weighted sum of this function $r(x) = 1$ and $r_t(x)$.

Eigenvector interpolation (*see* 2.2.)

The correlations $\mathbf{r}_0$ are derived from the local statistical field characteristics, homogeneity and isotropy need not be assumed. Even a constant variance is not required and instead of describing the statistical structure by correlations, covariances can be used. The coefficients $\mathbf{p}_0$ are then found from

$$\mathbf{p}_0 = \mathbf{S}^{m^{-1}}\,\mathbf{s}_0 \qquad \text{(A7)}$$

where $\mathbf{S}^m$ is the matrix of empirical covariances, $\mathbf{s}_0$ the vector of locally deduced covariances. In the case of near singularity of the matrix $\mathbf{S}^m$ as a consequence of high mutual covariances, $\mathbf{p}_0$ can be found by latent root regression, where the inversion of $\mathbf{S}^m$ is replaced by computation of the generalized inverse of rank L, lower than the order N of matrix $\mathbf{S}^m$ (Marquardt, 1970). The inverse of the true matrix $\mathbf{S}$ is obtained as

$$\mathbf{S}^- = \sum_{k=1}^{L} \lambda_k^{-1}\,\mathbf{e}_k\,\mathbf{e}'_k$$

where λ_k and $\mathbf{e}_k$ are respectively the k-th largest eigenvalue and associated eigenvector (length 1) of the symmetrical matrix $\mathbf{S}$, respectively; $\mathbf{e}_k$ is a column vector and $\mathbf{e}'_k$ its transposition to a row vector. The matrix $\mathbf{S}$ is thus approximated by the first L ones of N matrices $\lambda_k \mathbf{e}_k \mathbf{e}'_k$ which together describe the 'total variance'. The vector $\mathbf{s}_0$ of expected covariances between grid (interpolation) point and the monitoring stations could then be given by

$$\mathbf{S}_0 = \sum_{k=1}^{L} \lambda_k\, e_{k0}\,\mathbf{e}_k$$

where e_{k0} is the scalar value of the k-th eigenvector at the grid-point position, obtained by some local interpolation from the elements e_{ki} at the observation stations. The empirical matrix $\mathbf{S}^m$ can be considered as the sum of the true covariances $\mathbf{S}$ and the error variances, where the error covariances, as before, are assumed to be negligible:

$$\mathbf{S}^m = \mathbf{S} + \mathbf{I}h_i^2$$

Now $\mathbf{p}_0$ is found in a similar way as in Equation (A3b)

$$\mathbf{p}_0 = (\mathbf{S} + \mathbf{I}\overline{h_i^2})^-\,\mathbf{s}_0 = \sum_{k=1}^{L} (\lambda_k + \overline{h_i^2})^{-1}\,\mathbf{e}_k\,\mathbf{e}'_k\;\lambda_k\, e_{k0}\,\mathbf{e}_k$$

$$\mathbf{p}_0 = \sum_{k=1}^{L} \frac{\lambda_k}{(\lambda_k + \overline{h_i^2})}\, e_{k0}\,\mathbf{e}_k \qquad \text{(A8)}$$

So the coefficients p_{0i} are found from a linear combination of the eigenvectors of the matrix $\mathbf{S}^m$, which in the approximation used are equal to the eigenvectors of $\mathbf{S}$. Only vectors for which $\lambda_k \gg \overline{h_i^2}$, will contribute to $\mathbf{p}_0$. As the eigenvalues λ_k of the true covariance matrix $\mathbf{S}$ are unknown, L has to be choosen such that $\lambda_k/(\lambda_k + \overline{h_i^2}) \simeq 1$ for $k \leqslant L$ and $\simeq 0$ for $k > L$.

The smaller eigenvalues of the empirical matrix $\mathbf{S}^m$, which are of the same magnitude as $\overline{h_i^2}$, will not contribute to $\mathbf{p}_0$ and thus can be ignored.

A practical measure to determine the number of eigenvectors which are relevant for the interpolation, can be obtained by rewriting the interpolation error as

$$\overline{E_{0l}^2} = \overline{C_{0l}^2} - \sum_{k=1}^{L} \frac{\lambda_k^2}{\lambda_k + \overline{h_l^2}} e_{k0}^2 + \sum_{k=1}^{L} \frac{\lambda_k^2}{\lambda_k + \overline{h_l^2}} (e_{k0} - \hat{e}_{k0})^2 \quad \text{(A9)}$$

where $(e_{k0} - \hat{e}_{k0})$ is the discrepancy between the true value e_{k0} and the estimation $\hat{e}_{k0}$, obtained from the values e_{ki} at observation stations by some local interpolation. For an eigenvector analysis in which the values e_{k0} are known at all stations, this discrepancy can be computed and the value of k can be determined for which the third term in Equation (A9) becomes larger than the second one, i.e. $(e_{k0} - \hat{e}_{k0})^2 > e_{k0}^2$, indicating that no further reduction of $\overline{E_{0l}^2}$ can be expected by inserting vector k and possible consecutive vectors with smaller eigenvalues. These vectors apparently describe fluctuations on sub-network scale, by definition thus representing sampling errors, being irrelevant for interpolation.

As only the larger eigenvalues of $\mathbf{S}^m$ are taken into account, near-singularity, i.e., the existence of eigenvalues close to zero, does not result in computational instability as demonstrated by Equation (A8). Thus the coefficients $\mathbf{p}_0$ also can be computed if high mutual correlations (covariances) occur